

MODELING ANISOTROPIC PLASTICITY: 3D EULERIAN HYDROCODE SIMULATIONS OF HIGH STRAIN RATE DEFORMATION PROCESSES

Michael W. Burkett¹, Sean P. Clancy², Paul J. Maudlin³, and Kathleen S. Holian⁴

¹*Applied Physics Division, Primary Design and Assessment Group X-4*

²*Applied Physics Division, Integrated Physics Methods Group X-3*

³*Theoretical Division, Fluid Dynamics Group T-3*

⁴*Computing Communications and Networking Division, Scientific Software Engineering Group CCN-12
Los Alamos National Laboratory, Los Alamos, NM 87545*

Abstract. Previously developed constitutive models and solution algorithms for anisotropic elastoplastic material strength have been implemented in the three-dimensional Conejo hydrodynamics code. The anisotropic constitutive modeling is posed in an unrotated material frame of reference using the theorem of polar decomposition to obtain rigid body rotation. Continuous quadratic yield functions fitted from polycrystal simulations for a metallic hexagonal-close-packed structure were utilized. Simple rectangular shear problems, R-Value problems, and Taylor cylinder impact data were used to verify and validate the implementation of the anisotropic model. A stretching rod problem (involving large strain and high strain-rate deformation) was selected to investigate the effects of material anisotropy. Conejo simulations of rod topology were compared for two anisotropic cases.

INTRODUCTION

Accurate constitutive descriptions are required for high strain-rate deformation processes involving metals whose mechanical response shows significant directional dependence. The viability of utilizing anisotropic elastoplastic constitutive modeling to predict the large rigid body rotation and plastic deformation was shown previously (1). These calculations showed a large sensitivity to the yield function description for a hexagonal-close-packed material (high yield anisotropy). Constitutive models and solution algorithms for anisotropic elastoplastic material strength (2) developed for a Lagrangian (EPIC) continuum mechanics code have been implemented in the three-dimensional Conejo (3) code. Conejo was developed under the Accelerated Strategic Computing Initiative (ASCI) BLANCA code project.

HYDROCODE ARCHITECTURE

Conejo is an explicit, Eulerian continuum mechanics code that is used to predict formation processes associated with large material deformation at elevated strain-rates. Some special features of Conejo include a high-order advection algorithm, a material interface tracking scheme, and van Leer monotonic advection limiting. Conejo utilizes an object-oriented framework written in C++ called Tecolote. This framework is designed to facilitate the development and implementation of numerical and physical models that are used in hydrodynamic calculations. The Tecolote framework is built on the C++ POOMA library. POOMA or Parallel Object-Oriented Methods and Applications is an object-oriented framework for computational applications that require advanced parallel computers. POOMA provides Tecolote with fields (similar to Fortran-90 arrays) that



perform operations on parallel platforms efficiently store data in memory and streamline operations like divergence and gradient. The Blanca project team utilized many of these framework features during the implementation of the anisotropic plasticity model.

ANISOTROPIC PLASTICITY MODEL

The anisotropic constitutive modeling is posed in an unrotated material reference frame in order to satisfy constitutive modeling frame indifference. Constitutive modeling in this unrotated frame is convenient in that it can be performed while ignoring rigid body rotation as discussed below. Plasticity is assumed to be the dominant feature of our high-rate (10^4 to 10^7 s⁻¹) application problems of interest. As a result, we assume that the elastic part of the material response is isotropic. The anisotropic plastic potential or yield surface is represented with a general quadratic function (4) written in terms of the Cauchy stress and a fourth-order symmetric tensor:

$$f \equiv \underline{s} : \underline{\alpha} : \underline{s} - 2/3 \sigma^2 \quad (1)$$

where \underline{s} is a flow stress and the shape $\underline{\alpha}$ tensor expressed in Voigt-Mandel components has the form:

$$VM(\underline{\alpha}) = \begin{pmatrix} \alpha_{11} & \alpha_{12} & \alpha_{13} & \alpha_{14} & \alpha_{15} & \alpha_{16} \\ & \alpha_{22} & \alpha_{23} & \alpha_{24} & \alpha_{25} & \alpha_{26} \\ & & \alpha_{33} & \alpha_{34} & \alpha_{35} & \alpha_{36} \\ & & & \alpha_{44} & \alpha_{45} & \alpha_{46} \\ & & & & \alpha_{55} & \alpha_{56} \\ & & & & & \alpha_{66} \end{pmatrix} \quad (2)$$

The constitutive model equations are expressed in rate form since Conejo solves a set of hyperbolic time-dependent equations. The traditional isotropic strength formulation found in most explicit hydrocodes uses an objective stress rate, a von Mises yield function, some realistic flow stress function and the geometric method of radial return. Our approach uses polar decomposition of the deformation gradient in rate form to obtain the rigid body rotation. We then

rotate the symmetric part of the velocity gradient tensor (i.e., rate of deformation tensor) into an unrotated material frame, apply a geometric normal return solution scheme analogous to the radial return method to find the new stress state, and then rotate this stress back into the laboratory frame. The Euler-Rodrigues formulation is used to quantify the rigid body rotation in terms of a rotation angle and unit vector for better interpretation and subsequent advection. The model has been verified and validated on the simple rectangular shear problem, r-value problems and Taylor cylinder impact tests. The model has been applied to a stretching rod problem to investigate the effects of material anisotropy on plastic localization phenomena at strain rates of $\sim 10^4$ s⁻¹. Conejo predictions of the topology were compared for two anisotropic cases.

R-VALUE PROBLEM

Consider a rectangular bar uniaxially loaded in the 1 direction (long direction of bar) without initial specimen rotation, the r-value of interest is r_{23} which is the ratio of the plastic deformation rates in two orthogonal directions perpendicular to the load direction (5). We performed three r-value calculations using a set of tantalum (Ta) shape factors, α . Our computational model for this problem consisted of a 0.635 by 0.635-cm cross-section rectangular bar that is placed in uniaxial tension by applying a 20 m/s uniform velocity field. The r-value was evaluated at the center (in terms of length and width) of the specimen segment. Steady state uniaxial stress conditions are required in order to evaluate the r-values. Each calculation assumed that the bar was uniaxially loaded in tension along the 1 axis. The calculations assumed rigid body rotations about the 1, 2, and 3 axes of $\theta = 45$ degrees, respectively.

Analytical r-value expressions in terms of orthotropic shape coefficients for uniaxial loading in the 1 direction for the three cases involving rigid body rotation about the 1, 2, and 3 axes respectively are:

$$r_{23} = \frac{\frac{(\alpha_{13} - \alpha_{12}) \cos 2\theta + \alpha_{11}}{\alpha_{11} + (\alpha_{12} - \alpha_{13}) \cos 2\theta} \cdot \frac{4\alpha_{22} + 4(\alpha_{23} - \alpha_{12}) \cos 2\theta}{\alpha_{23} - 4\alpha_{13} + \alpha_{12} + 2\alpha_{55} + (-\alpha_{23} - 4\alpha_{13} - \alpha_{12} - 2\alpha_{55}) \cos 4\theta} \cdot \frac{\alpha_{33} + 4\alpha_{12} - 2\alpha_{66} - \cos 4\theta(\alpha_{33} - 4\alpha_{12} - 2\alpha_{66})}{4((\alpha_{13} - \alpha_{23}) \cos \theta - \alpha_{33})}}{(3a,b,c)}$$

The theoretical r_{23} values for Ta for the three loading cases are 1.00, 0.7015, 1.290, respectively. Figure 1 shows the axes and angle definitions relative to the bar orientation and Figure 2 shows a comparison of the calculated (as a function of time) and the theoretical r -value for the three cases. The calculated values oscillate about the theoretical values as the stress state in the bar rings about the uniaxial stress condition.

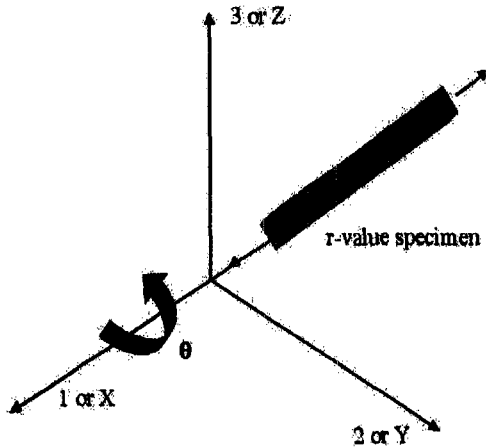


FIGURE 1. Axes selections and computational model for r -value calculations. Case one rotation depicted.

TAYLOR CYLINDER PROBLEM

Taylor impact testing has been historically used to validate constitutive modeling in continuum mechanics codes (6). Comparisons of time resolved plastic wave propagation and final deformation shapes (cylinder side profiles and footprints) can be used to validate model predictions. We have performed preliminary anisotropic model validation calculations of a Ta Taylor Cylinder test. Also, we have performed isotropic cylinder impact test calculations so that

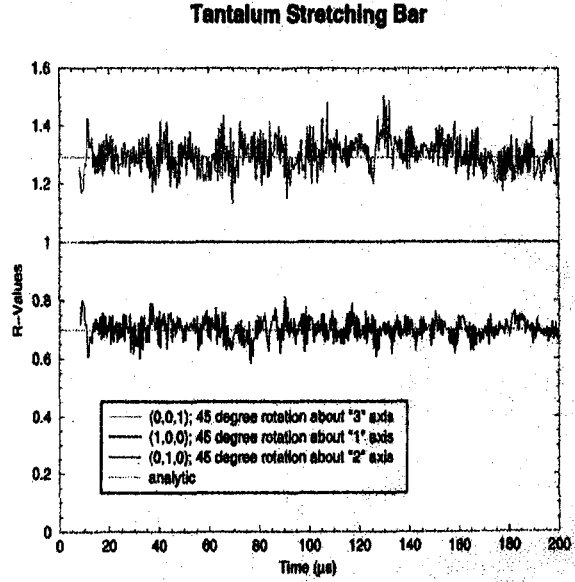


FIGURE 2. Comparison of theoretical and calculated r -values.

comparisons of the deformation characteristics associated with anisotropic and isotropic modeling assumptions can be made. The cylinder was 0.381-cm in radius and 2.54-cm long traveling at 175 m/s. Figure 3 contrasts the cylinder footprints for Ta isotropic and anisotropic yield surfaces after the plastic deformation process has completed (~80 μ s). The figures also show the magnitude of the Euler-Rodrigues angle (in radians) and vector orientation. These vectors are oriented in a counter-clockwise pattern indicating that the impact end of the cylinder is plastically deforming in the radial direction. For the isotropic case, the magnitude of the Euler-Rodrigues angle indicates that the deformation gradient is uniform: no circumferential rotation gradient and correspondingly no dependence upon the yield surface orientation, applied load direction or initial material texture. Radial gradients in the Euler-Rodrigues angle indicate that most of the rigid rotation is concentrated at the perimeter of the footprint for both cases. In the anisotropic calculation, the variation in magnitude of the Euler-Rodrigues angle along the circumference of the cylinder shows that the deformation is non-uniform and is controlled by the interaction of the yield surface orientation, loading direction, and

initial rigid body rotation. The plastic flow is larger along the Y-axis because the flow stress is softer in the Y-direction given the yield surface shape for this material. In this calculation, the strong axis of the yield surface was initially oriented along the Z-axis (perpendicular to the loading direction (X-axis)). This configuration produces an elliptical footprint with some flattening along 45° lines.

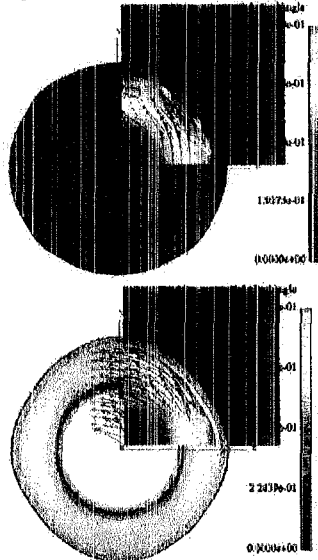


FIGURE 3. Taylor Cylinder calculations showing Euler-Rodriguez angle and vectors for an isotropic (top) and anisotropic (bottom) yield surface description for Ta. Linear gradients in rotation angle (radians) from 0.0 to 0.771 (isotropic) and 0.0 to 0.9135 (anisotropic) are realized.

STRETCHING ROD PROBLEM

Plastic tensile instability (necking) is an important consideration for a variety of stretching rod deformation processes. A potential stabilization mechanism for the rod necking problem is yield anisotropy. The stability of a stretching metal rod has dependencies that include the material flow stress (σ), density (ρ), axial strain rate ($\dot{\epsilon}$), rod radius (a), and the initial distribution of geometric perturbations (7,8). Romero (8) defines the following isotropic dimensionless number $\Gamma(t)$ based upon these parameters:

$$\Gamma(t) = \sqrt{3} \rho \dot{\epsilon}^2(t) a^2(t) / \sigma(t) \quad (4)$$

Perturbations are stable (no necks should develop on the rod surface) for $\Gamma(t) > 1$. As the rod is stretched, $\Gamma(t)$ decreases. For $\Gamma(t) < 1$, perturbations can become unstable. Note that the stability equation indicates a softer flow stress produces a more stable rod geometry. Our numerical study of rod topology consists of a comparison of two anisotropic cases (0° and 90° initial rotation about the 1 or X axis). The Ta rod has an initial radius of 0.213-cm, an initial length of 0.852-cm and an average strain rate of $\sim 10^4$ 1/s. Figure 4 shows that the deformed cross section shapes are not circular but elliptical. The calculated topologies show a strong sensitivity to the yield surface coefficients (α) or yield surface orientation for the tensile plastic instability problem.

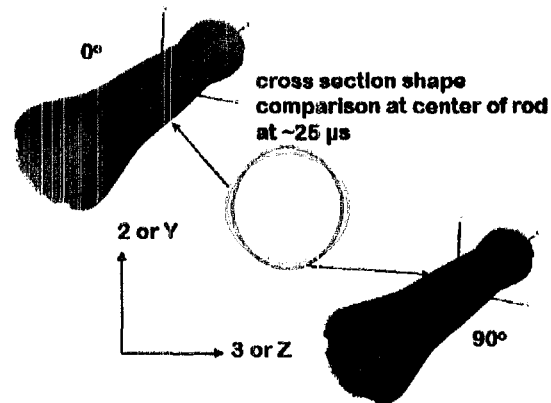


FIGURE 4. Comparison of rod cross sections at ~ 25 s for 0° and 90° initial rotation angles about the X axis.

REFERENCES

1. Clancy, S. P., Burkett, M. W., Maudlin, P. J., J. Phys. IV France 7 Colloq. C3 (DYMAT 97), 735-740 (1997).
2. Maudlin, P. J. and Schiffrer S. K., *Comput. Methods Appl. Mech. Engrg.* 131 (1996) 1-30.
3. Holian, K. S., et al., Proceeding of the Conference on Numerical Simulations and Physical Processes related to Shock Waves in Condensed Media, Oxford, England, September 1997.
4. Maudlin, P. J., Bingert, J. F., Gray III, G. T., *J. J. Plasticity*, accepted for publication, May 2001.
5. Hill, R., *The Mathematical Theory of Plasticity* (Oxford University Press, London, (1950).
6. Taylor, G. I., I. Theoretical Considerations. *Proc. R. Soc. Lond. A* 194, 289 (1948).
7. Walsh, J. M., *J. Appl. Phys.*, 56 (7) 1 (1984).
8. Romero, L. A., *J. Appl. Phys.*, 65, 3006 (1989).